Current Biology *18*, 963–968, July 8, 2008 DOI 10.1016/j.cub.2008.05.043

Report

Integration of Bimodal Looming Signals through Neuronal Coherence in the Temporal Lobe

Joost X. Maier,[1] Chandramouli Chandrasekaran,[2] and Asif A. Ghazanfar[1,2,*]
[1]Max Planck Institute for Biological Cybernetics
Spemannstrasse 38
72076 Tuebingen
Germany
[2]Neuroscience Institute and Department of Psychology
Princeton University
Princeton, New Jersey 08540

Summary

The ability to integrate information across multiple sensory systems offers several behavioral advantages, from quicker reaction times and more accurate responses to better detection and more robust learning [1]. At the neural level, multisensory integration requires large-scale interactions between different brain regions—the convergence of information from separate sensory modalities, represented by distinct neuronal populations. The interactions between these neuronal populations must be fast and flexible, so that behaviorally relevant signals belonging to the same object or event can be immediately integrated and integration of unrelated signals can be prevented. Looming signals are a particular class of signals that are behaviorally relevant for animals and that occur in both the auditory and visual domain [2–4]. These signals indicate the rapid approach of objects and provide highly salient warning cues about impending impact. We show here that multisensory integration of auditory and visual looming signals may be mediated by functional interactions between auditory cortex and the superior temporal sulcus, two areas involved in integrating behaviorally relevant auditory-visual signals [5, 6]. Audiovisual looming signals elicited increased gamma-band coherence between these areas, relative to unimodal or receding-motion signals. This suggests that the neocortex uses fast, flexible intercortical interactions to mediate multisensory integration.

Results and Discussion

Behavioral studies in primates, including humans, have shown strong attentional biases for detecting and responding to auditory [3, 7], visual [2], and multisensory [8, 9] looming signals, as compared to receding signals. Looming percepts and behavioral reactions can be induced by using rising-intensity sounds in the auditory domain [10] and rapidly expanding disks in the visual domain [2]. At the neural level, response biases to such signals are reflected in auditory cortex [11] and the superior temporal sulcus (STS) [12, 13] of the monkey, and human imaging studies have recently shown that these two areas are part of a large-scale network involved in coordinating behavioral responses [14, 15]. Moreover, both areas have been shown to be involved in auditory-visual (AV) integration [5, 6]. In the present study, we investigated the role of intercortical synchronization of neuronal activity in auditory cortex and the STS as a mechanism for the integration of auditory and visual looming signals.

While our monkey subjects fixated centrally, we simultaneously recorded local field potential (LFP) activity, representing the responses of populations of synchronized neurons from the lateral belt area of auditory cortex and the upper bank of the STS to auditory, visual, and AV looming and receding signals (see Experimental Procedures). The stimuli are shown in Figure 1A: Auditory looming and receding signals were rising- and falling-intensity complex tones, and visual stimuli were solid black disks, expanding (looming) or contracting (receding) on a gray background [3, 8]. Intensity change and expansion/contraction was smooth over a dynamic period of 1000 ms. A schematic time course of the stimuli is shown in Figure 1B. Stimuli started and ended with a 300 ms static period, allowing us to exclude transient neural onset and offset responses from the analysis of the response to the dynamic period of the stimuli [11]. AV stimuli could be either congruent or incongruent. Incongruent looming signals consist of auditory looming and visual receding stimuli; incongruent receding signals consist of auditory receding and visual looming stimuli. All statistical analyses were performed on the mean response during the dynamic period after it was normalized to the baseline period (500 ms before stimulus onset) unless otherwise indicated.

Black traces in Figure 1C show the raw LFP responses from one example cortical site in auditory cortex and the simultaneously recorded LFP signal from one cortical site in the STS in response to auditory and visual looming stimuli. In auditory cortex, the auditory response is characterized by short-latency, transient onset responses. Visual stimuli usually elicited no onset responses in auditory cortex. In the STS, both visual and auditory stimuli elicited short-latency onset responses, as expected given its polysensory properties [16]. In the present case, our primary interest lies in the dynamic portion of the stimulus. During this period, the amplitude of the raw LFP signal was not differentially modulated in the different conditions. However, examining the same signals in the frequency domain revealed a sustained increase in oscillatory activity in response to the looming stimuli [11]. Auditory and visual looming signals elicited an increase in oscillatory activity in auditory cortex and the STS, respectively (Figure 1C, spectrograms). This increase was sustained throughout the duration of the dynamic period and was most pronounced in the gamma-frequency range (45–90 Hz). Receding stimuli did not elicit a clear sustained increase in oscillatory activity in auditory cortex [11] or the STS (data not shown). Figures 2A and B show the mean population gamma-band power in response to the dynamic period of looming and receding stimuli, relative to baseline (auditory cortex: n = 50 cortical sites; STS: n = 67 cortical sites). Overall, looming stimuli elicited a greater response compared to receding stimuli in both auditory cortex ($p < 0.001$) and the STS ($p = 0.029$). This bias for looming over receding signals is consistent with previous findings in auditory cortex [11, 15] and the STS [12–14] and probably reflects the greater behavioral relevance of detecting rapidly approaching objects as compared to receding objects.

*Correspondence: asifg@princeton.edu

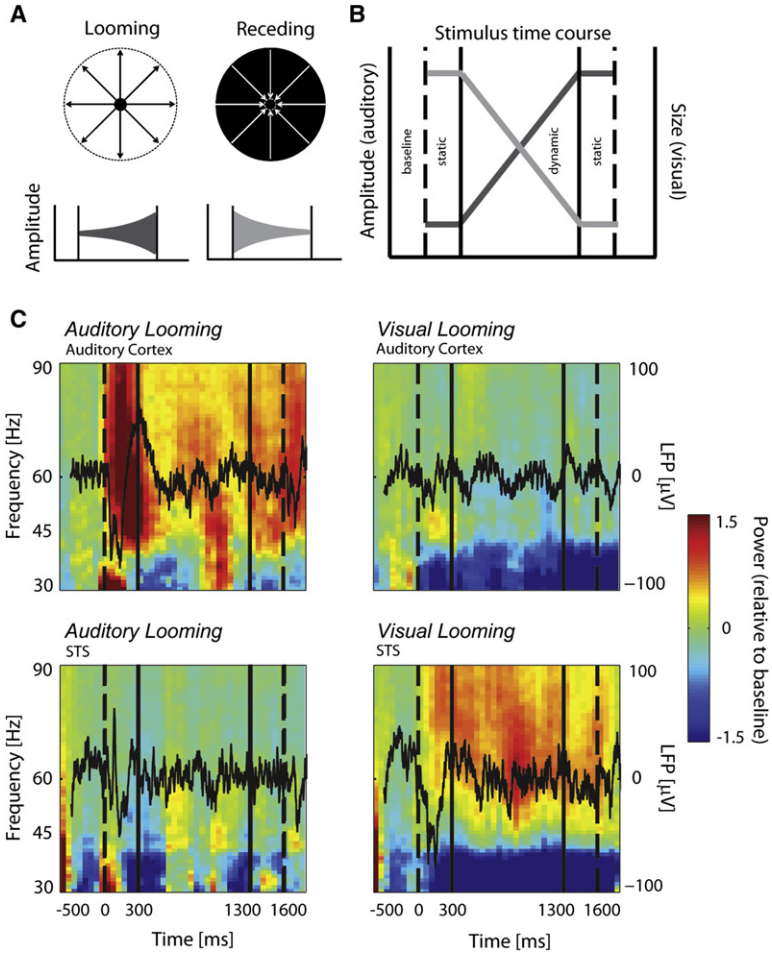

Figure 1. Looming Signals Evoke Sustained Oscillatory Activity in the Gamma Band in Auditory Cortex and the STS

(A) Visual (upper) and auditory (lower) stimuli. Visual stimuli consisted of a black disk symmetrically expanding (looming) or contracting (receding) on a gray background. Auditory stimuli were rising- (looming) and falling- (receding) intensity complex tones.

(B) Schematic time course of the stimuli. The dynamic portion of the stimuli was preceded and followed by a 300 ms static period so that we could exclude neural onset and offset responses. Dashed vertical lines represent onset and offset of the stimuli. Solid vertical lines mark the start and end of the dynamic portion of the stimuli.

(C) Time-amplitude representation of raw LFP signals (black traces), overlaid on corresponding spectrograms, simultaneously recorded from example cortical sites in auditory cortex and the STS, in response to auditory and visual looming stimuli. Traces and spectrograms represent the mean response over 32 trials per condition.

One possibility is that integration of auditory and visual looming signals results in increased power in auditory cortex, the STS, or both. However, we found no evidence for differential modulation during multisensory versus unisensory conditions: Gamma power in auditory cortex was mainly modulated by auditory signals (Figure 2A), whereas gamma power in the STS was mainly modulated by visual signals (Figure 2B). An ANOVA showed a significant effect of condition (auditory, visual, congruent AV, and incongruent AV) in auditory cortex ($p = 0.019$) and the STS ($p = 0.017$). Pairwise comparisons showed no significant differences in gamma power between the multisensory (congruent and incongruent) and auditory conditions in auditory cortex, nor differences between the multisensory and visual conditions in the STS (t test: $p > 0.05$). Thus, in terms of response magnitude (i.e., power modulations), the data provide no evidence for multisensory integration in the responses of these two areas. Sustained gamma-power increases in response to looming stimuli in auditory cortex were exclusively modulated by auditory signals. Sustained gamma power in the STS was exclusively modulated by visual signals, even though the STS showed transient responses to both auditory and visual signals at their onsets (Figure 1C). In light of this finding, we regard the activity recorded from the STS during the dynamic period of the stimuli as unisensory visual, perhaps reflecting activity from unimodally responsive neuronal populations interspersed among multisensory populations [17].

An alternative mechanism to power changes is multisensory integration via modulation of temporal interactions between the two areas [18]. Temporally correlated neuronal activity is a mechanism for establishing functional interactions between separate neuronal populations [19]. Figure 3A shows LFP activity, recorded simultaneously from auditory cortex (top panel) and the STS (middle panel), during one trial in the congruent AV looming condition. Within single trials, we observed multiple periods (100–200 ms) of highly correlated gamma-band activity recorded from the two areas (Figure 3A, bottom panel). We used coherence as a measure of the strength of such correlations. Figure 3B shows the coherence, relative to baseline, of a single pair of cortical sites in the four different looming conditions. Coherence was increased in the gamma band and highest during the dynamic period of congruent AV looming stimuli. Figure S1A (available online) shows the average coherogram across the population of cortical pairs for all looming conditions. Figure 3C shows the mean gamma coherence during the dynamic period of the looming stimuli for the population of pairs that had significant coherence in at least one of the conditions ($n = 98$ pairs of cortical sites). Significance was determined with a permutation test (see Experimental Procedures). Looming stimuli elicited greater increases in coherence as compared to receding stimuli ($p = 0.019$). An ANOVA showed a significant effect of condition ($p < 0.001$). Comparisons of the different conditions revealed that gamma coherence was selectively increased in response to congruent AV looming stimuli, relative to all other looming conditions (congruent AV versus auditory: $p = 0.004$; congruent AV versus visual: $p = 0.002$; and congruent AV versus incongruent AV: $p < 0.001$). Increased gamma coherence in the congruent AV looming condition is possibly confounded by the fact that both auditory cortex and the STS have increased power in the gamma range. To address this issue, we first looked at whether there was a relationship between increases in gamma coherence in pairs of recording sites and increases in gamma power at the constituent recording sites. In Figure 3D, we plotted gamma coherence, relative to baseline, against gamma power, relative to baseline (geometric mean of gamma power in the STS site and the auditory

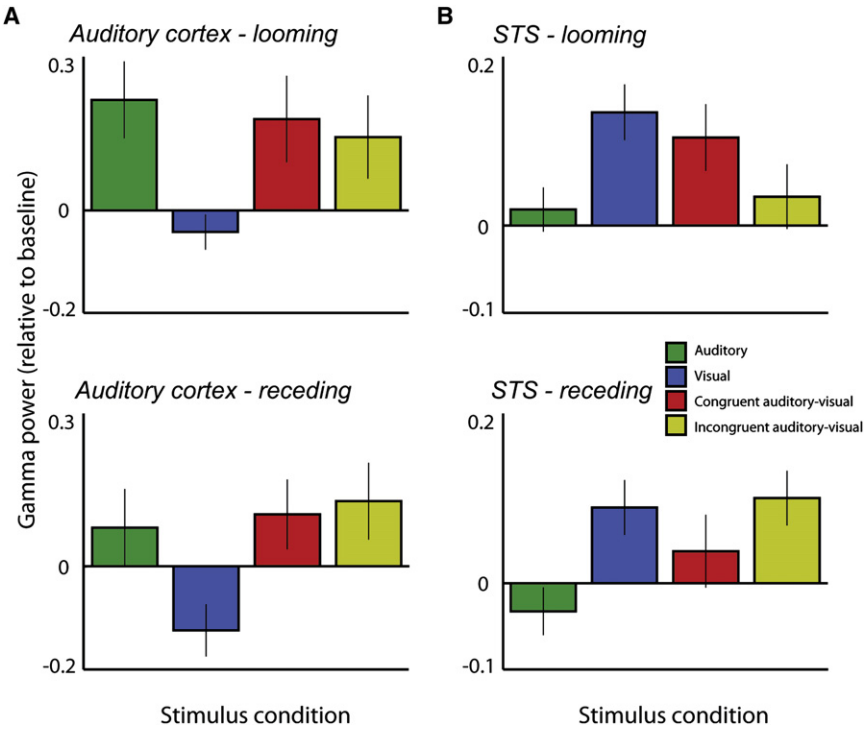

Figure 2. Auditory Cortex and the STS Respond to Auditory and Visual Looming Signals, Respectively

(A and B) Mean gamma-band power during the dynamic portion of looming and receding stimuli in the different conditions, relative to baseline, averaged across cortical sites in auditory cortex (n = 50; [A]) and the STS (n = 67; [B]). Error bars represent ± 1 SEM. Note that incongruent looming signals consist of auditory looming and visual receding stimuli, and incongruent receding signals consist of auditory receding and visual looming stimuli.

cortex site) for all pairs of recording sites that showed increased gamma power in response to the congruent AV looming condition (n = 66) [20]. There was no significant linear relationship between the two measures (r^2 = 0.017, p = 0.301). Second, we calculated phase synchrony between the two areas. Phase synchrony is a measure of phase-locking between signals, and it is independent of the amplitude [21]. Figure 3E shows mean phase synchrony in the gamma band during the dynamic period of the looming stimuli for the same pairs as shown in Figure 3C (n = 98). Overall, phase synchrony shows the same pattern over conditions as observed for coherence. Statistical analyses also showed similar effects, although some comparisons did not quite reach our alpha level of 5% (looming versus receding: p = 0.056; ANOVA with factor condition: p = 0.063; congruent AV versus auditory: p = 0.043; congruent AV versus visual: p = 0.009; and congruent AV versus incongruent AV: p = 0.015). Average phase synchrony over time and frequency for all looming conditions can be found in Figure S1B. Taken together, we find that both the correlation measure and, to some degree, the phase synchrony measure indicate that the observed increases in coherence are at least partly independent of power changes and reflect enhanced phase-locking of the LFP signals in auditory cortex and the STS.

To address the directionality of the coherence between auditory cortex and the STS, we computed the phase spectrum (see Supplemental Data) [18, 22]. The change of the phase angle as a function of frequency provides an estimate of the delay between the two structures. The slope of the regression line provides an estimate of the delay between the two structures' oscillations. Figure 4A shows two examples of phase angle as a function of frequency from two different cortical pairs. The left panel shows a slope of 0.0125 rad/Hz, which equates to 1.99 ms, whereas the right panel shows a slope of 0.0312 rad/Hz, which equates to 4.97 ms. The slopes are positive, showing that auditory cortex lags the STS. Figure 4B shows a distribution of slopes across our sample of cortical pairs. The mean slope was 0.015 rad/Hz, which translates to a delay of 2.38 ms (one-sample t test: p = 0.0026). These analyses suggest that the coherence between auditory cortex and the STS is mediated by feedback projections from the STS to auditory cortex. Moreover, a consistent phase difference between auditory cortex and the STS also suggests that increased coherence indeed reflects phase coupling of oscillations in these two areas.

The present results show enhanced coherent neuronal activity between auditory cortex and the STS, specifically during perception of congruent AV looming signals (although it does not preclude interactions between other structures), and suggest that neuronal coherence may act as a mechanism for establishing fast, dynamic, and selective functional connections between separate populations of neurons representing signals from different sensory modalities. Such auditory cortical-STS coherence might result in more efficient communication between these areas and frontoparietal networks [22–24], resulting in better-coordinated responses to looming events [14, 15, 25]. The lack of similar neuronal coherence in responses to congruent but receding audiovisual signals may seem odd in light of the fact that both the STS and auditory cortex consistently show integrative responses to other forms of congruent artificial multisensory stimuli [26, 27]. However, the pattern of our results matches behavioral results, which show that monkeys exhibit a strong attentional preference for visual looming signals when presented simultaneously with auditory looming signals but no analogous preference for congruent receding signals [8].

Previous studies have hypothesized a role for multisensory STS feedback in modulating neural responses in auditory cortex [5, 27–31]. Direct communication between strictly unisensory areas has also been suggested as a mechanism for multisensory integration [32, 33]. Our data are a curious mix of the two ideas. The present study shows interactions between auditory cortex and unimodal visual neuronal populations within the generally multisensory STS. Thus, although STS is generally considered a multisensory convergence zone, our data revealed that, beyond the onset responses to our specific auditory and visual stimuli, the sustained gamma-band responses were purely visual. This suggests that polysensory responses in the STS are limited to the onsets, are frequency-band specific, and/or are dependent upon the nature of the stimuli.

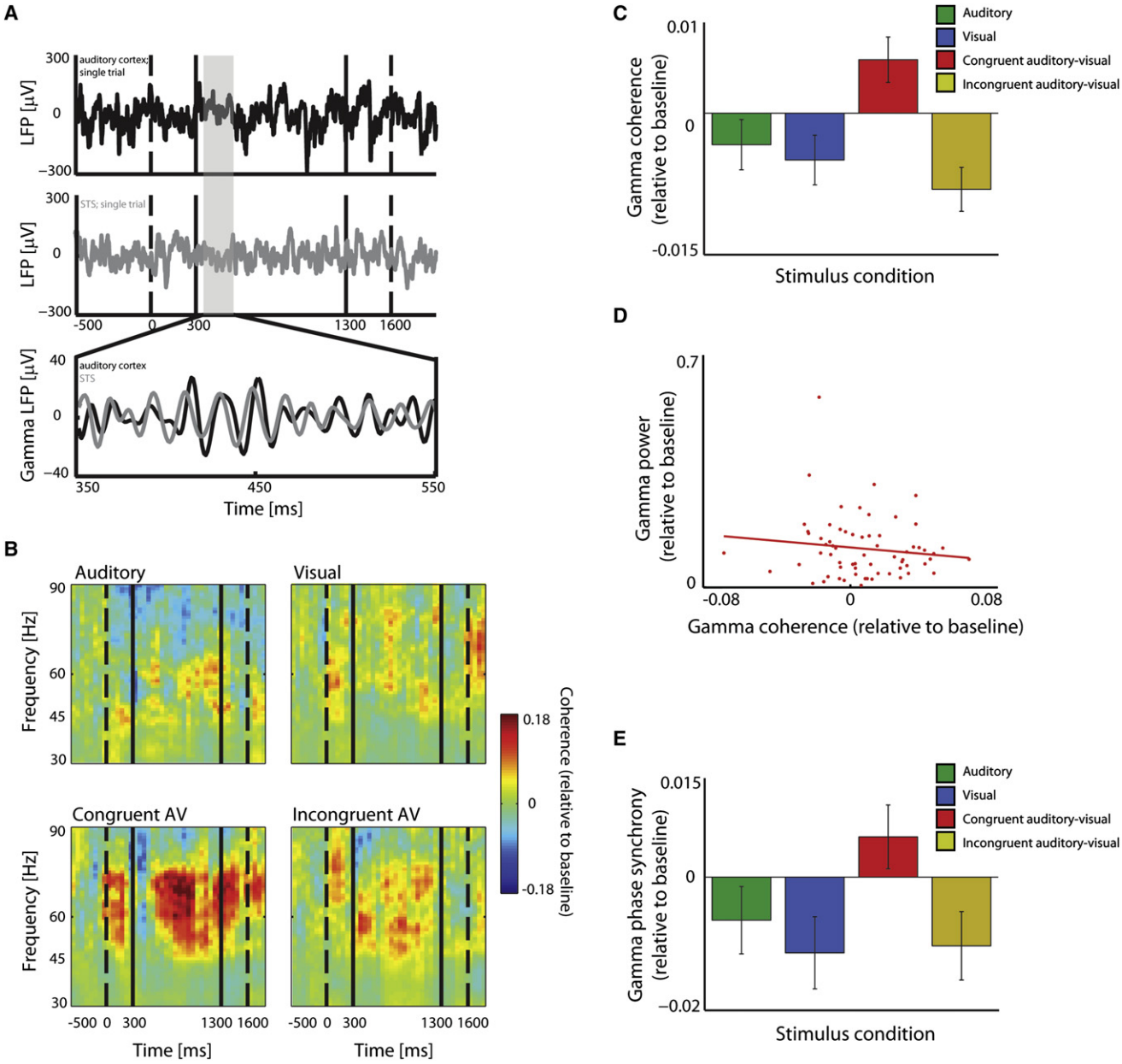

Figure 3. Gamma-Band Coherence Is Selectively Increased during Congruent Auditory-Visual Stimulation

(A) LFP signals simultaneously recorded from auditory cortex and the STS during a single trial in the congruent AV looming condition. The portions indicated by the box are filtered between 45 and 90 Hz and overlaid (bottom trace).

(B) Coherence, relative to baseline, between LFP signals recorded from one example pair of cortical sites in auditory cortex and the STS, in the auditory, visual, congruent AV, and incongruent AV conditions. Coherograms represent the mean across 32 trials per condition.

(C) Gamma-band coherence, relative to baseline, in the auditory, visual, congruent AV, and incongruent AV conditions, averaged across pairs of cortical sites (n = 98). Error bars represent ±1 SEM.

(D) Gamma-band coherence, normalized to baseline, plotted against total gamma-band power, normalized to baseline (geometric mean of the gamma power in the STS site and the auditory cortex site), for all pairs of recording sites that showed increased gamma-band power in response to the congruent AV looming condition (n = 66). The solid line represents linear regression.

(E) Phase synchrony in the gamma band, relative to baseline, in the auditory, visual, congruent AV, and incongruent AV conditions, averaged across pairs of cortical sites (n = 98). Error bars represent ±1 SEM.

Experimental Procedures

Two adult male rhesus monkeys (*Macaca mulatta*) were used as subjects in the experiments. All experiments were performed in compliance with the guidelines of the local authorities (Regierungspraesidium) and the European Community (EU VD 86/609/EEC) for the care and use of laboratory animals.

Stimuli

Auditory stimuli, rising- and falling-intensity complex tones, were generated with SoundForge and Adobe Audition. The amplitude envelopes either rose or fell quadratically over a period of 1000 ms. Visual stimuli were generated with the Psychophysics Toolbox [34] and consisted of black disks, exponentially expanding or contracting over 1000 ms on a gray background. All stimuli started and ended with a 300 ms static period flanking the

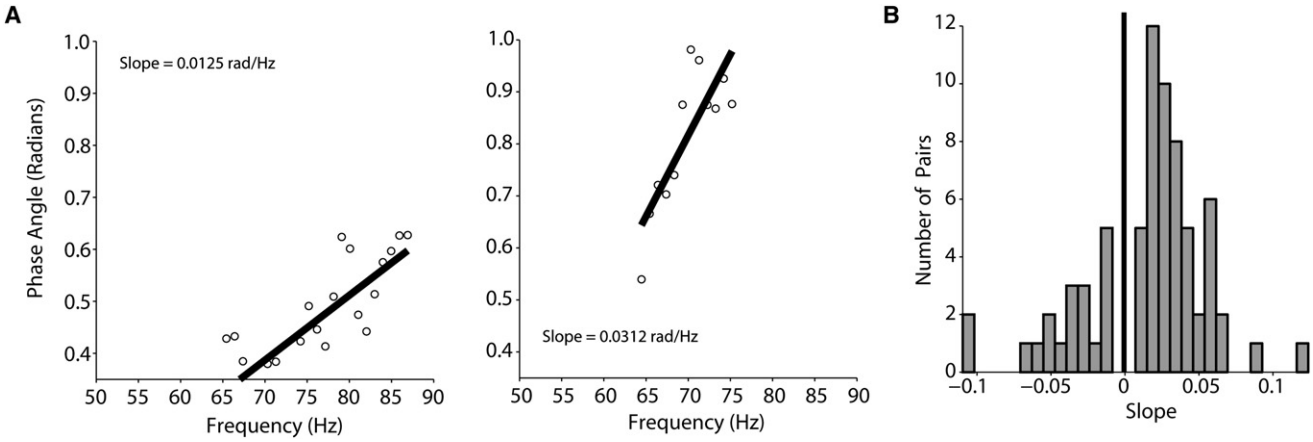

Figure 4. Phase Spectra for Gamma-Band Coherence during the Auditory-Visual Looming Condition

(A) Two phase spectra for two different cortical pairs. The measurements were taken during the dynamic period of the stimulus presentation. In both examples, the slopes are positive, suggesting that STS activity leads auditory cortical activity.

(B) The distribution of slopes across the population of cortical pairs in our sample. The majority of slopes were positive.

dynamic interval, resulting in stimuli with a total duration of 1600 ms. Initial intensity/size was varied.

Behavioral Paradigm

A trial began with the appearance of a central fixation spot. Subjects were required to fixate this spot within a 1 or 2 degree radius. After 500 ms of fixation, a stimulus appeared for 1600 ms. The stimulus could either be (1) an auditory stimulus alone; (2) a visual stimulus alone; (3) a congruent auditory-visual stimulus; or (4) an incongruent AV stimulus (an auditory looming stimulus with a visual receding stimulus, or vice versa). Subjects had to maintain fixation throughout the duration of the stimulus. Successful completion of a trial resulted in a juice reward. During each recording session, between 20 and 40 repetitions of each stimulus were presented. Details of stimulus presentation are included in the Supplemental Data.

Data Collection

Data for all events relevant to the experiment, such as stimulus information and eye position, were stored. Signals from the electrodes were amplified, filtered between 1 and 5000 Hz, acquired with a sampling rate of 20.8 kHz, and stored for offline analysis. Physiological identification of auditory cortex and the STS is described in the Supplemental Data.

Data Analysis

All data analysis was performed in Matlab. To obtain LFP activity, we filtered the raw neural signal between 1 and 300 Hz (fourth order, zero-phase, bidirectional Butterworth filter) and resampled it at 1000 Hz. For LFP analyses, we applied multitaper spectral analysis to estimate spectral power and coherence [35, 36] with the Chronux suite of routines developed in Matlab for neural analyses (http://www.chronux.org). For time-frequency analysis of spectral power and coherence, we used nine Slepian data tapers on a 250 ms sliding window (shifted by 50 ms) [35, 37, 38]. Phase synchrony for each pair of recording sites was calculated by taking the circular mean of the phase difference in each time-frequency bin over trials [21]. For population analyses, we only used pairs of recording sites that showed significant coherence in at least one of the conditions. To determine significance, we generated a random distribution of coherence values by calculating the coherence between the LFP signals from all simultaneously recorded pairs of electrodes (n = 105) after pairing trials in random order. This procedure was repeated five times for each looming condition, resulting in 2100 random coherence values. Mean coherence values in the gamma range during the dynamic period of the stimuli obtained from the real (nonrandomized) data that exceeded the 95% confidence limit of the distribution of mean values obtained from the randomized coherence data (0.0711) were considered significant. Mean coherence ranged from 0.0428 to 0.3694 (mean ± standard deviation: 0.1148 ± 0.0563). For all subsequent analyses, data were normalized to baseline before averaging across cortical sites.

Supplemental Data

Additional Experimental Procedures and one figure are available at http://www.current-biology.com/cgi/content/full/18/13/963/DC1/.

Acknowledgments

This study was conducted under the auspices of Dr. Nikos Logothetis. Without his encouragement and generosity, this work would not have been possible. We thank Christoph Kayser and Kari Hoffman for valuable discussions and Hjalmar Turesson for help with the recordings. We also gratefully acknowledge the efforts and insights of an anonymous reviewer. This work was supported by the Max Planck Society (J.X.M. and A.A.G.) and by Princeton University's Training Program in Quantitative and Computational Neuroscience (NIH R90 DA023419-02) (C.C.).

Received: February 7, 2008
Revised: May 22, 2008
Accepted: May 23, 2008
Published online: June 26, 2008

References

1. Rowe, C. (1999). Receiver psychology and the evolution of multicomponent signals. Anim. Behav. *58*, 921–931.
2. Schiff, W., Caviness, J.A., and Gibson, J.J. (1962). Persistent fear responses in rhesus monkeys to the optical stimulus of "looming". Science *136*, 982–983.
3. Ghazanfar, A.A., Neuhoff, J.G., and Logothetis, N.K. (2002). Auditory looming perception in rhesus monkeys. Proc. Natl. Acad. Sci. USA *99*, 15755–15757.
4. Neuhoff, J.G. (1998). Perceptual bias for rising tones. Nature *395*, 123–124.
5. Ghazanfar, A.A., Maier, J.X., Hoffman, K.L., and Logothetis, N.K. (2005). Multisensory integration of dynamic faces and voices in rhesus monkey auditory cortex. J. Neurosci. *25*, 5004–5012.
6. Barraclough, N.E., Xiao, D., Baker, C.I., Oram, M.W., and Perrett, D.I. (2005). Integration of visual and auditory information by superior temporal sulcus neurons responsive to the sight of actions. J. Cogn. Neurosci. *17*, 377–391.
7. Freiberg, K., Tually, K., and Crassini, B. (2001). Use of an auditory looming task to test infants' sensitivity to sound pressure level as an auditory distance cue. British Journal of Developmental Psychology. *19*, 1–10.
8. Maier, J.X., Neuhoff, J.G., Logothetis, N.K., and Ghazanfar, A.A. (2004). Multisensory integration of looming signals by rhesus monkeys. Neuron *43*, 177–181.

9. Gordon, M.S., and Rosenblum, L.D. (2005). Effects of intrastimulus modality change on audiovisual time-to-arrival judgments. Percept. Psychophys. *67*, 580–594.
10. Rosenblum, L.D., Carello, C., and Pastore, R.E. (1987). Relative effectiveness of three stimulus variables for locating a moving sound source. Perception *16*, 175–186.
11. Maier, J.X., and Ghazanfar, A.A. (2007). Looming biases in monkey auditory cortex. J. Neurosci. *27*, 4093–4100.
12. Hietanen, J.K., and Perrett, D.I. (1996). A comparison of visual responses to object- and ego-motion in the macaque superior temporal polysensory area. Exp. Brain Res. *108*, 341–345.
13. Anderson, K.C., and Siegel, R.M. (1999). Optic flow selectivity in the anterior superior temporal polysensory area, STPa, of the behaving monkey. J. Neurosci. *19*, 2681–2692.
14. Seifritz, E., Neuhoff, J.G., Bilecen, D., Scheffler, K., Mustovic, H., Schachinger, H., Elefante, R., and Di Salle, F. (2002). Neural processing of auditory looming in the human brain. Curr. Biol. *12*, 2147–2151.
15. Bach, D.R., Schachinger, H., Neuhoff, J.G., Esposito, F., Di Salle, F., Lehmann, C., Herdener, M., Scheffler, K., and Seifritz, E. (2007). Rising sound intensity: An intrinsic warning cue activating the amygdala. Cereb. Cortex *18*, 145–150.
16. Bruce, C., Desimone, R., and Gross, C.G. (1981). Visual properties of neurons in a polysensory area in superior temporal sulcus of the macaque. J. Neurophysiol. *46*, 369–384.
17. Beauchamp, M.S., Argall, B.D., Bodurka, J., Duyn, J.H., and Martin, A. (2004). Unraveling multisensory integration: Patchy organization within human STS multisensory cortex. Nat. Neurosci. *7*, 1190–1192.
18. Schoffelen, J.M., Oostenveld, R., and Fries, P. (2005). Neuronal coherence as a mechanism of effective corticospinal interaction. Science *308*, 111–113.
19. Fries, P. (2005). A mechanism for cognitive dynamics: Neuronal communication through neuronal coherence. Trends Cogn. Sci. *9*, 474–480.
20. Srinivasan, R., Russell, D.P., Edelman, G.M., and Tononi, G. (1999). Increased synchronization of neuromagnetic responses during conscious perception. J. Neurosci. *19*, 5435–5448.
21. Lachaux, J.P., Rodriguez, E., Martinerie, J., and Varela, F.J. (1999). Measuring phase synchrony in brain signals. Hum. Brain Mapp. *8*, 194–208.
22. Saalmann, Y.B., Pigarev, I.N., and Vidyasagar, T.R. (2007). Neural mechanisms of visual attention: How top-down feedback highlights relevant locations. Science *316*, 1612–1615.
23. Womelsdorf, T., Fries, P., Mitra, P.P., and Desimone, R. (2006). Gamma-band synchronization in visual cortex predicts speed of change detection. Nature *439*, 733–736.
24. Womelsdorf, T., Schoffelen, J.M., Oostenveld, R., Singer, W., Desimone, R., Engel, A.K., and Fries, P. (2007). Modulation of neuronal interactions through neuronal synchronization. Science *316*, 1609–1612.
25. Field, D.T., and Wann, J.P. (2005). Perceiving time to collision activates the sensorimotor cortex. Curr. Biol. *15*, 453–458.
26. Lakatos, P., Chen, C.-M., O'Connell, M.N., Mills, A., and Schroeder, C.E. (2007). Neuronal oscillations and multisensory interaction in primary auditory cortex. Neuron *53*, 279–292.
27. Noesselt, T., Rieger, J.W., Schoenfeld, M.A., Kanowski, M., Hinrichs, H., Heinze, H.-J., and Driver, J. (2007). Audiovisual temporal correspondence modulates human multisensory superior temporal sulcus plus primary sensory cortices. J. Neurosci. *27*, 11431–11441.
28. Calvert, G.A. (2001). Crossmodal processing in the human brain: Insights from functional neuroimaging studies. Cereb. Cortex *11*, 1110–1123.
29. Schroeder, C.E., and Foxe, J.J. (2002). The timing and laminar profile of converging inputs to multisensory areas of the macaque neocortex. Cognitive Brain Research *14*, 187–198.
30. van Atteveldt, N., Formisano, E., Goebel, R., and Blomert, L. (2004). Integration of letters and speech sounds in the human brain. Neuron *43*, 271–282.
31. McDonald, J.J., Teder-Salejarvi, W.A., Di Russo, F., and Hillyard, S.A. (2003). Neural substrates of perceptual enhancement by cross-modal spatial attention. J. Cogn. Neurosci. *15*, 10–19.
32. Ghazanfar, A.A., and Schroeder, C.E. (2006). Is neocortex essentially multisensory? Trends Cogn. Sci. *10*, 278–285.
33. Driver, J., and Noesselt, T. (2008). Multisensory interplay reveals crossmodal influences on 'sensory-specific' brain regions, neural responses, and judgments. Neuron *57*, 11–23.
34. Brainard, D.H. (1997). The Psychophysics Toolbox. Spat. Vis. *10*, 433–436.
35. Pesaran, B., Pezaris, J.S., Sahani, M., Mitra, P.P., and Andersen, R.A. (2002). Temporal structure in neuronal activity during working memory in macaque parietal cortex. Nat. Neurosci. *5*, 805–811.
36. Mitra, P.P., and Pesaran, B. (1999). Analysis of dynamic brain imaging data. Biophys. J. *76*, 691–708.
37. Scherberger, H., Jarvis, M.R., and Andersen, R.A. (2005). Cortical local field potential encodes movement intentions in the posterior parietal cortex. Neuron *46*, 347–354.
38. Palanca, B.J., and DeAngelis, G.C. (2005). Does neuronal synchrony underlie visual feature grouping? Neuron *46*, 333–346.

Supplemental Data

Integration of Bimodal Looming Signals through Neuronal Coherence in the Temporal Lobe

Joost X. Maier, Chandramouli Chandrasekaran and Asif A. Ghazanfar

Supplemental Experimental Procedures

Surgical Preparation

For each of the two subjects, we used preoperative magnetic resonance imaging (4.7 T magnet, 500 μm slices) to identify the stereotaxic coordinates of auditory cortex and to model a 3D skull reconstruction. From these skull models, we constructed custom-designed, form-fitting titanium headposts and recording chambers. The subjects each underwent sterile surgery for the implantation of a scleral search coil [S1], headpost, and recording chamber. The inner diameter of the recording chamber was 19 mm and was vertically oriented to allow a perpendicular approach to the surface of the superior temporal plane [S2, S3].

Stimulus Presentation

The subjects were head restrained and sat in a primate chair in front of a 21 inch color monitor at a distance of 94 cm. A speaker (JBL control 1X) was placed on both sides of the monitor. Two speakers were used to reduce the spatial mismatch between the visual and the auditory signals. Auditory stimuli were presented at two different intensity ranges, from 68 to 80 dB SPL or 50 to 68 dB SPL, as measured with a Brüel & Kjær sound level meter at a distance of 94 cm (A-weighted). The size of the visual stimuli also had two different ranges, from ~5 degrees (fully contracted) to ~10 degrees (fully expanded) or ~2 degrees to ~5 degrees. Experiments were conducted in a double-walled sound-attenuating booth lined with echo-attenuating foam.

Data Collection

For recording of neural events, we employed a custom-made multielectrode drive that allowed us to move up to eight electrodes independently. Electrodes were arranged in a 4 × 2 staggered array, covering 12 mm in the anterior-posterior dimension and 1.5 mm in the medial-lateral dimension. Guide tubes (25 gauge) were used to penetrate the tissue growth and dura overlying the cortex. Electrodes were glass-coated tungsten wire with impedances between 1 and 3 MΩ measured at 1 kHz. Amplification and filtering were done with a combination of Alpha Omega Engineering hardware, custom-designed software, and a National Instruments board (BNC-2090).

Identification of Auditory Cortex and the STS

Electrodes were lowered until multiunit activity (MUA) could be reliably driven by auditory stimuli. Search stimuli included pure tones, FM sweeps, noise bursts, clicks, and monkey vocalizations. For each recording site, we made frequency-tuning curves by using the MUA responses to 25 pure tone pips (100 Hz–21 kHz) presented at an intensity of 72 dB. In both subjects, we discerned a coarse tonotopic map representing high-to-low frequencies in the caudal-to-rostral direction. Such a map is identified as primary auditory cortex (A1). When the electrode array was moved 2 mm in the lateral direction, the same rough tonotopic map was observed, but complex stimuli (noise, clicks, and vocalizations) generally elicited much stronger responses than pure tones, indicating that the electrodes were in lateral belt auditory cortex [S4, S5] adjacent to A1 (the middle lateral belt area, ML [S6]). The core and lateral-belt regions are also distinguished by their sensitivity to multisensory inputs [S7, S8]. These physiological criteria serve only as a rough guide, and it is likely that some of our electrodes were occasionally placed in rostrally adjacent regions of the lateral belt. The STS was defined as the layer of cortex directly below area ML of auditory cortex. The two layers of cortex were separated by ~2 mm of white matter in which no spiking activity could be detected. This area of the upper bank of the STS corresponds to the superior temporal polysensory area (STP) [S9, S10].

Estimating the Phase Spectrum

During instances in which the coherence was significantly different from baseline, we obtained the phase differences by taking the argument of the cross-spectrum. The cross-spectrum is the product of the conjugate of the Fourier transform of the first signal multiplied by the second Fourier transform. This result leads to a phase subtraction.

In our case, we obtained the cross-spectrum by multiplying the conjugate of the auditory cortex spectrum by the STS spectrum. The cross-spectrum provides the phase-angle difference between the two structures and can be converted into a time delay. The cross-spectrum between the two signals is given as follows: Let F_{STS} denote the complex spectrum of the STS signal and F_{AUD} denote the complex spectrum of the auditory-cortex signal. Traditionally, and in the implementation of the coherency we use, the cross spectrum is defined as

$$C = F^{*}_{AUD} F_{STS}$$

$$\tilde{C}(f) = r_{AUD} r_{STS} e^{i(\theta_{STS} - \theta_{AUD})}$$

where the asterisk denotes the conjugation. The argument of this complex number provides the phase lag between the auditory cortex and STS signals. We fit a regression line to these phase angles as a function of frequency. The slope of this line A is then used to estimate the delay between the two signals. The delay is given as

$$\Delta = \frac{-1000A}{2\pi}$$

where A is the slope of the phase angle plotted against frequency. When the Δ is positive (i.e., the slope is negative), auditory cortical activity can be said to precede the STS activity by a constant delay. For each frequency, it means that the phase of the auditory signal is larger than the phase of the STS signal.

When the values of the phase are positive and increasing (which is what our data show), the STS phase is larger than the auditory-cortex phase. That is, the difference, $\theta_{STS} - \theta_{AUD}$, is positive and increasing with frequency. This means that the STS gamma oscillations lead auditory cortical oscillations.

In essence, we estimated the phase angles on a pair-by-pair basis during the time regions within the stimulus period that showed significant coherence (tested with bootstrap error bars). We then fitted regression lines, as a function of frequency, to each time point (within the region of significant coherence) and then selected the time point with the maximal regression fit. We took the mean delays afforded by these pairs and used those to estimate the delay between auditory cortex and STS (see Figure 4).

Supplemental References

S1. Robinson, D.A. (1963). A method of measuring eye movement using a scleral search coil in a magnetic field. IEEE Trans. Biomed. Eng. *10*, 137–145.

S2. Pfingst, B.E., and O'Connor, T.A. (1980). A vertical stereotaxic approach to auditory cortex in the unanesthetized monkey. J. Neurosci. Methods *2*, 33–45.

S3. Recanzone, G.H., Guard, D.C., and Phan, M.L. (2000). Frequency and intensity response properties of single neurons in the auditory cortex of the behaving macaque monkey. J. Neurophysiol. *83*, 2315–2331.

S4. Rauschecker, J.P., and Tian, B. (2004). Processing of band-passed noise in the lateral auditory belt cortex of the rhesus monkey. J. Neurophysiol. *91*, 2578–2589.

S5. Rauschecker, J.P., Tian, B., and Hauser, M. (1995). Processing of complex sounds in the macaque nonprimary auditory cortex. Science *268*, 111–114.

S6. Kaas, J.H., and Hackett, T.A. (2000). Subdivisions of auditory cortex and processing streams in primates. Proc. Natl. Acad. Sci. USA *97*, 11793–11799.

S7. Lehmann, C., Herdener, M., Esposito, F., Hubl, D., di Salle, F., Scheffler, K., Bach, D.R., Federspiel, A., Kretz, R., Dierks, T., et al. (2006). Differential patterns of multisensory interactions in core and belt areas of human auditory cortex. Neuroimage *31*, 294–300.

S8. Ghazanfar, A.A., Maier, J.X., Hoffman, K.L., and Logothetis, N.K. (2005). Multisensory integration of dynamic faces and voices in rhesus monkey auditory cortex. J. Neurosci. *25*, 5004–5012.

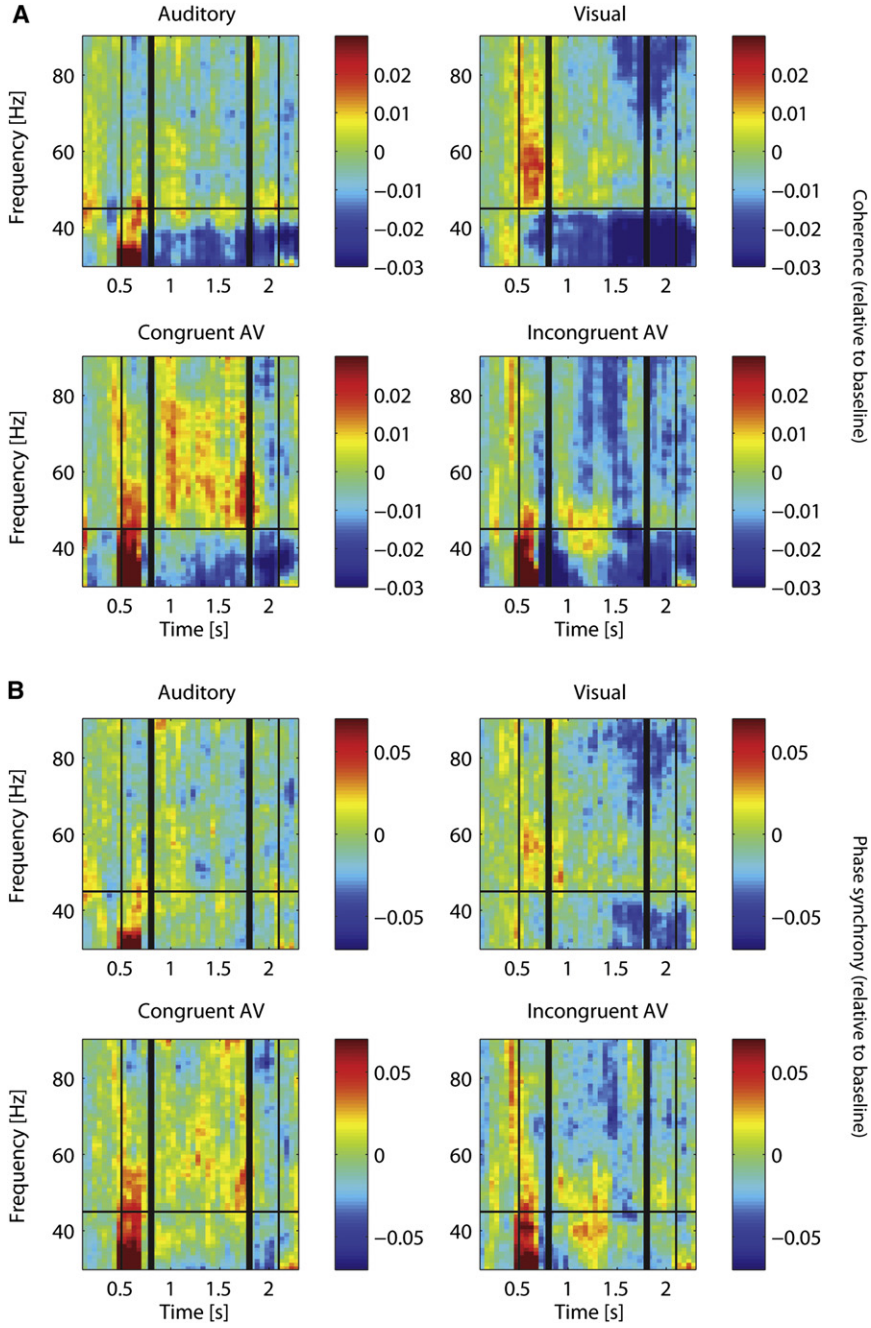

Figure S1. Average Coherogram and Phase Synchrony across the Population of Cortical Pairs for All Looming Conditions

Coherence (A) and phase synchrony (B) over time and frequency, relative to baseline, between LFP signals recorded from auditory cortex and the STS, in the auditory, visual, congruent AV, and incongruent AV looming conditions. Data represent the mean across 98 pairs of recording sites.

S9. Bruce, C., Desimone, R., and Gross, C.G. (1981). Visual properties of neurons in a polysensory area in superior temporal sulcus of the macaque. J. Neurophysiol. *46*, 369–384.

S10. Desimone, R., and Gross, C.G. (1979). Visual areas in the temporal cortex of the macaque. Brain Res. *178*, 363–380.